Electrification Pathways for Sustainable Syngas Production: A Comparative Analysis for Low-Temperature Fischer-Tropsch Technology

Afroditi Kourou [a], Simon De Langhe [a], Lander Nelis [a], Yannick Ureel [a], Matthijs Ruitenbeek [b], Kees Biesheuvel [b], Ronald Wevers [b], Yi Ouyang [a,*], Kevin M. Van Geem [a,*]

[a] Laboratory for Chemical Technology, Ghent University, Technologiepark-Zwijnaarde 125, B-9052, Zwijnaarde, Belgium

[b] Dow Benelux B.V., P.O. Box48, 4530 AA Terneuzen, Netherlands

[*] Corresponding author. Laboratory for Chemical Technology, Ghent University, Technologiepark-Zwijnaarde 125, B-9052, Zwijnaarde, Belgium. E-mail address: kevin.vangeem@ugent.be (K.M. Van Geem).

[*] Corresponding author. Laboratory for Chemical Technology, Ghent University, Technologiepark-Zwijnaarde 125, B-9052, Zwijnaarde, Belgium. E-mail address: yi.ouyang@ugent.be (Y. Ouyang).

Keywords: Electrified chemicals, Techno-economic analysis, Electrolysis, Combined steam and dry reforming of methane, Autothermal reforming

Abstract

The electrification of chemical processes holds promise for a sustainable and climate-neutral chemical industry. This study explores pathways for electrifying syngas production, targeting its utilization in low-temperature Fischer-Tropsch (LT-FT) technology with a hydrocarbon production capacity of 222 kton/yr. Three electrified scenarios are juxtaposed against a reference case of autothermal reforming of biomethane. In the first two scenarios, H_2 is produced via water electrolysis, with CO obtained either through CO_2 electrolysis (Electrolysis case) or electrified reverse water-gas shift (E-rWGS case). The third scenario leverages captured CO_2 and biomethane for electrified combined steam and dry reforming of methane (CSDRM case), exhibiting the lowest net emissions of 0.50 $ton_{CO2}/ton_{product}$. All electrified scenarios achieve net negative emissions under the EU's 2030 target of 40% overall renewable energy production. A detailed techno-economic analysis reveals significant feasibility challenges with the Electrolysis, E-rWGS, and CSDRM cases exhibiting a Levelized Cost Of Production (LCOP) of $501, $457, and $251 per barrel (bbl) of Fischer-Tropsch crude, respectively. Future projections suggest considerable capital cost reductions for electrolyzers, potentially rendering the Electrolysis case feasible, particularly under extremely low electricity prices of 3.3 $/MWh. Careful consideration of green electricity and CO_2 utilization scenarios is vital for implementing CO_2-negative technologies effectively.

1. Introduction

In December 2015, the Paris Agreement was ratified, signifying a unified stance among the United Nations to cap global warming below 2 °C, with a preference for 1.5 °C, compared to pre-industrial

levels. Achieving this goal necessitates significant cuts in greenhouse gas (GHG) emissions, thereby placing pressure on the industrial sector to play its part in this collective endeavor [1]. The chemical industry, accounting for 7% of global GHG emissions, stands as one of the main industry sectors with high energy consumption and associated GHG emissions [2]. The reduction of GHG emissions in the chemical industry can be achieved via a combination of routes such as carbon capture (CC) technologies, reducing emissions through process intensification, transitioning to a circular economy, and electrification of energy-intensive processes with green electricity [3-5]. With the availability of renewable energy rapidly increasing, more options for the electrification of the chemical industry arise [3]. Nonetheless, the amount of green electricity required for such a venture is currently not available. Various strategies exist for the implementation of electrification [1]. Direct electrification involves the utilization of green electricity as a thermal energy source for chemical processes, thereby replacing the energy provided by burning conventional carbon-based fuels [3, 6]. Additionally, electricity can be used to upgrade waste heat via heat pumps in order to minimize energy losses and maximize efficiency [6]. Another path for electrification is the direct electrochemical production of chemicals, such as hydrogen (H_2) through water electrolysis [6]. Electrification can also be applied to produce other commodity chemicals through electrochemical synthesis instead of thermochemical synthesis [7, 8].

Synthetic fuels can serve as intermediate energy carriers to gradually integrate the, constantly increasing, intermittent renewable energy provision [9]. They also serve a purpose as reagents for the synthesis of various chemicals. Fischer-Tropsch (FT) synthesis provides a sustainable way to produce synthetic fuels and chemicals via the catalytic conversion of syngas, a mixture of H_2 and carbon monoxide (CO), into a mixture of (liquid) hydrocarbons. This study investigates different possible routes for electrifying the production of syngas used in the FT technology starting from renewable carbon sources and thereby integrating complementary processes into a cohesive system. The exothermicity of the FT process allows coupling with emerging technologies, leading to a higher thermal efficiency of the synthetic hydrocarbons production [10]. Therefore, an overview of possible sustainable syngas production technologies is presented in order to identify the most suitable routes towards electrification. The sustainability of the produced syngas is ensured through the use of sustainable feedstocks such as captured CO_2 and biomethane, while direct and indirect (scope 1-2-3) emissions are taken into account. Biomethane is produced via biogas upgrading and is considered an attractive alternative to natural gas, as it has a similar heating value but also a high potential to reach negative GHG emissions [11]. Biogas is a sustainable and efficient energy source that consists primarily of CH_4 and CO_2 along with some other gas traces [11]. However, the use of biomethane as a feedstock in this study was crucial due to the high CO_2 content in the biogas as well as the inclusion of trace amounts of sulfur compounds that lead to catalyst poisoning [11]. According to IEA, the cost of biomethane includes both the cost of biogas production and the cost required for upgrading [12].

Syngas acts as a flexible starting point for the production of valuable base chemicals and consists primarily of H_2 and CO and typically traces of CO_2. This mixture can be used for the production of methanol, olefins (via methanol-to-olefins), ammonia, and other valuable products. The H_2:CO-ratio in syngas is a crucial factor for processes that utilize syngas as a feedstock as it influences the reactions and selectivity towards the end-products. In FT, this ratio affects the choice of catalyst, as for Fe-based catalysts a low ratio (0.5-1.2) is possible due to the presence of the WGS functionality, while for Co-based catalysts, a higher ratio (close to 2) needs to be selected [13]. Steam Methane Reforming (SMR) is the most common method to convert methane (CH_4) and water (H_2O) into syngas [14] and relies on natural gas as its primary feedstock [15]. The overall reaction is strongly endothermic and is operated at high temperatures (850-900 °C) and moderate pressures (up to 35 bar) [16]. From an environmental perspective, an SMR reformer is marked by a high carbon footprint, producing 7.5-10.0 kg CO_2 per kg of H_2 produced [15]. One way to provide the heat necessary for the SMR reactions is by employing the autothermal reforming (ATR) process, which combines the reactions occurring in the SMR with partial oxidation reactions. In the ATR technology, the partial oxidation of methane provides the thermal energy required for the methane reforming reaction while maintaining a high energy efficiency [11, 17, 18]. ATR shows great potential for a lower carbon footprint compared to the conventional SMR [19, 20], even though it typically has a lower H_2 production yield [11]. Moreover, ATR is suited for producing syngas with an H_2:CO ratio of 1.5-3, as needed for LT-FT technology [19]. SMR typically produces syngas with a high H_2 yield, resulting in an H_2:CO ratio of around 3 [21]. Therefore, ATR serves as the benchmark technology for sustainable syngas production for the purposes of this study. In order to evaluate the potential of syngas electrification, different routes for syngas production are proposed emphasizing the technologies that are presently prevalent or demonstrate high potential in the energy landscape.

One pathway to produce sustainable syngas via electrification is the separate production of H_2 and CO. According to the International Energy Agency (IEA), the H_2 demand is expected to increase from 94 million metric tons (Mt) in 2021 to 115 Mt in 2030, while the low-emission H_2 production is forecasted to substantially increase from 1 Mt to a range of 16-24 Mt [22]. H_2 has a variety of applications, as it can be used as a feedstock for chemical processes, and as a medium for energy storage [6]. H_2 can be utilized in a fuel cell, which is an electrochemical device that converts H_2 and O_2 into water while producing electricity [11]. Fuel cells can produce electricity efficiently with very low pollution emissions [11]. Produced H_2 is typically categorized by color based on the feedstock, processing technology, and associated GHG emissions [23]. For instance, green H_2 is produced from water electrolysis using renewable energy, while grey H_2 is produced from natural gas reforming, which can be considered blue H_2 when coupled with carbon capture and storage [24]. Based on the current state regarding the trade-off between cost-effectiveness and GHG emissions, hydrogen production from hydrocarbons develops as the predominant method [23].

Currently, SMR stands as the predominant method for H_2 production [15], with an energy efficiency in the range of 74–85% [16] and a high carbon footprint as mentioned above. Green H_2, on the other side, is produced by H_2O electrolysis, where the direct splitting of water in high purity H_2 and oxygen (O_2) is achieved by applying an electrical current originated from renewable sources such as wind and solar energy [16, 25]. Three major technologies for H_2O electrolysis are discussed: alkaline water electrolyzers (AWE), proton exchange membrane (PEM) cells, and solid oxide electrolysis cells (SOEC) [26]. AWE is a commercially available technology that employs an aqueous KOH solution [27] and operates within a temperature range of 60-90 °C and a pressure range of 1-30 bar [28]. These types of electrolyzers typically operate with an energy efficiency in the range of 60%-80% [26, 29]. PEM operates under similar temperature conditions as AWE but in a higher pressure range of up to 85 bar [27]. PEM electrodes utilize noble metals such as Pt, Ir, and Ru as active materials making it a more expensive reactor technology compared to AWE [28, 30]. Nevertheless, PEM achieves a higher energy efficiency of 80% [26], while compared to AWE, it demonstrates an improved dynamic operation but has lower durability [28]. In contrast to AWE and PEM technologies, SOEC operates at elevated temperatures in the range of 500-1000 °C, demonstrating very high energy efficiency of up to 100% [31]. SOEC technology has the advantage of using non-noble metal catalysts. Nonetheless, it is not commercialized yet, as it comes with high costs and low durability due to exposure to high temperatures [28]. Hydrogen can be also produced through water splitting by means of photo-electrolysis and thermolysis [32]. In photo-electrolysis, semiconductors are used as photocatalysts in a photoelectrochemical cell to produce H_2 with solar energy, which constitutes the highest advantage of the technology [32]. Thermolysis is a solar thermal technique that splits the H_2O into H_2 and O_2 through high temperatures [32]. However, both technologies are currently associated with high costs and lower efficiency compared to water electrolysis [32]. Biomass gasification also provides a promising, well-established approach for sustainable production of hydrogen-rich syngas in a cost-effective, efficient and environmental way [33]. Current limitations however persist regarding catalyst deactivation, required energy and variety in feedstock composition, leading to the need for optimal development and selection of catalyst, operating parameters, and reactor type [33].

The other key component of syngas, CO, can be produced from CO_2 via various pathways. One possible path that has been broadly explored is the conversion of CO_2 to CO via the reverse water-gas shift (rWGS) reaction. RWGS is an endothermic reaction that is thermodynamically favored at high temperatures and involves the conversion of CO_2 and H_2 into CO and H_2O [34]. If excess H_2 is used and water and CO_2 are removed, the process leads to a mixture of CO and H_2 [34]. At lower temperatures, other side reactions are favored, such as the Sabatier reaction, methanation, and the Boudouard reaction, all resulting in a decrease in CO yield [34]. At present, considerable efforts are taking place in developing thermally stable catalysts to enhance selectivity towards CO at lower temperatures [35]. Active metals such as Cu or Ni have emerged due to their relatively low cost compared to noble metals and high

activity and selectivity, even though Cu-oxide and Ni-oxide tend to deactivate at high temperatures [36]. The development of alternative metal-based catalysts is being explored. For instance, the use of Mo_2C catalyst is another promising catalyst enhancing the CO_2 conversion and CO yield [37, 38]. The development of a thermal catalyst for low-temperature rWGS that could be applicable for integration with the FT reactor for a two-step conversion of CO_2 in a single reactor would be of significant interest [34]. Nevertheless, the rWGS is not practiced on an industrial scale yet as a standalone process [36]. Brown et. al assessed the environmental impact of the process, showing that it is indeed possible to achieve a net CO_2 consumption by using blue or green sources of H_2 and captured CO_2 without taking into account emissions from process heating [36]. From an economic standpoint, the primary impediment is the price of green H_2. However, it is anticipated that green H_2 prices will considerably reduce to below 4 \$/kg H_2 by 2040 [39], creating opportunities for CO generation via the rWGS reaction.

An alternative route for CO production is through the direct electrochemical reduction of CO_2. The electrochemical CO_2 reduction reaction (CO_2RR) process can be considered a utilization technique for converting captured CO_2 into sustainable fuels and chemicals using renewable energy [40]. The process has gained a lot of attention for its potential for practical CO_2 reduction, controllability, and optimization [40, 41]. To meet industrial requirements, the development of efficient electrolyzers is necessary [41]. Notably, the electroreduction of CO_2 is a complex process due to the high stability of the molecule, leading to low energy efficiencies [42]. Various methods have been proposed, with high-temperature electrolysis in SOEC emerging as the sole approach nearing commercialization [43]. Nevertheless, the technology is facing many challenges in terms of selectivity and activity. A deeper understanding of the reaction mechanism is needed to improve the electrocatalysts [44], while focus should be also given to the design of multi-stack CO_2 electrolysis cells [45].

Besides a separate production of H_2 and CO, direct syngas production processes are also a possibility. Dry reforming of methane (DRM) has been developed on a commercial scale to produce CO and H_2 from CH_4 and CO_2. However, undesired CO_2 can still be formed due to the WGS reaction, while other side reactions such as methane decomposition and the Boudouard reaction occur as well [46]. A major downside of DRM for syngas production for LT-FT is that it provides an H_2:CO-ratio of 0.8-1.0 [47]. Moreover, one of the main drawbacks of DRM has been the coke formation that leads to catalyst deactivation [48]. The development of catalysts suitable to commercialize the technology has been a huge challenge [46]. Apart from designing novel catalyst supports and promoters, coke formation can be potentially suppressed by adding another oxidizing reactant, such as H_2O to the feedstock [48]. In the presence of H_2O, surface carbon can gasify into gaseous products, reducing the catalyst deactivation [48]. This is a valid alternative that integrates the SMR and DRM into an advanced process named combined steam and dry reforming of methane (CSDRM). This process relies on CO_2 sequestration, offering the potential to result in a positive environmental impact [49, 50]. CSDRM merges the benefits of DRM and SMR resulting in a high H_2:CO-ratio. Depending on the steam to methane ratio, an H_2:CO-

ratio between 1-10 can be achieved. Thermodynamic CSDRM simulations have been conducted to identify the optimum conditions for suppressing carbon deposition while ensuring high conversion yields and a desired H_2:CO-ratio [51, 52]. The main drawback of the process is the high sensitivity to catalyst deactivation due to carbon deposition [50, 51]. Therefore, substantial efforts have been devoted to identifying the appropriate catalyst for the system, with the interest being mainly focused on the use of Ni-based catalysts [52].

In this work, a comparative analysis of sustainable electrified syngas production is performed focusing on the economic and CO_2 emissions impact. The reference year for the CO_2 emissions stemming from the electricity grid is 2023 at the EU level[53]. A conventional ATR serves as a benchmark here, where biomethane is processed to ensure the input of renewable carbon. This is compared to a total of three high-potential cases which are identified for the electrified syngas production. The overall target for all cases is to achieve an H_2:CO-ratio of 2.15. The "Electrolysis" case refers to the use of electrolyzers to produce H_2 from H_2O, and CO from CO_2. Specifically, the AWE technology has been chosen for water electrolysis, and the SOEC for CO_2 reduction. The "E-rWGS" case studies the potential of the electrified reverse water-gas shift reaction for CO production combined with AWE technology for H_2 production. The H_2 produced is used both as a feedstock for the rWGS and in the syngas composition to obtain the desired H_2:CO-ratio. The "CSDRM" case refers to the use of electrified CSDRM technology for syngas production, utilizing biomethane as well. An overview of the different cases is presented in Table 1

Table 1. Overview of the selected cases for syngas production.

Case no.	Case Name	Technology	Product
Reference	ATR	Autothermal reforming (ATR)	Syngas
1	Electrolysis	Alkaline Water Electrolyzer (AWE)	H_2
		Solid Oxide electrolysis Cells (SOEC)	CO
2	E-rWGS	Alkaline Water Electrolyzer (AWE)	H_2
		Reverse water-gas shift (rWGS)	CO
3	CSDRM	Combined steam and dry reforming of biomethane (CSDRM)	Syngas

2. Methodology

2.1. General basis of Design

The basis of design follows the outline of a typical FT plant across all cases. The feedstock was converted into a syngas stream in the syngas generation section followed by the FT reactor where syngas was subsequently converted into a mixture of hydrocarbons (FT crude). The annual syngas (in terms of H_2 and CO) capacity was targeted at 500 kton, aligning with industrial scale norms. This would result in an annual production of 222 kton of hydrocarbons, or equivalent to 25.5 ton per hour, assuming an annual time-on-stream of 8700 hours.

2.1.1. Feedstock

Table 2 provides details on the assumed available feedstock prices along with their conditions. In line with the study's sustainability focus, biomethane has an average price of 19 $/MMBtu [12]. CO_2 originated from carbon capture facilities with a relatively modest cost of 29 $/ton [54], assuming that it was locally captured and used, while the O_2 stream was derived from a cryogenic air separation unit (ASU), with a cost of 90 $/ton [55]. The FT-crude price was determined based on the levelized cost of production (LCOP), a metric that is elaborated in the following section.

Table 2. Feedstock conditions and prices.

Feedstock	Temperature (°C)	Pressure (bar)	Price
Oxygen	0.1	4.7	90 $/ton
Biomethane	40	40	19 $/MMBtu
Water	20	1	3.99 $/ton
Carbon dioxide	120	1	29 $/ton

2.1.2. Utilities

Natural gas is widely used for heat production. However, it is associated with undesired CO_2 emissions, and, therefore, the heating of the reactors in the electrified cases was achieved by electrical heating. A full pinch analysis was performed to achieve heat integration using the Elsevier Pinch Analysis Tool including all heating and cooling duties [56]. A minimum temperature approach of 10°C was assumed, and a correction factor of 90% was applied to ensure practicality. After heat integration was completed, the remaining required heat duty was delivered by assuming the combustion of natural gas with a boiling efficiency of 85%. Electricity was also available to all cases to power compressors and pumps. The prices and associated CO_2 emissions of the utilities are summarized in Table 3. The electricity and natural gas prices have been derived from the average values in the period between 2018 and 2022 for non-household consumers in the EU [57, 58]. The CO_2 emissions associated with electricity generation were assessed for the year 2023 at the EU level [53].

Table 3. Utilities prices and associated emissions.

Utility	Price	CO_2 emissions (g_{CO2}/kWh)
Natural gas	38.8 $/MWh	181
Electricity	113 $/MWh	242
Cooling water (at 15 °C)	0.050 $/ton	-

2.2. Process description

The process of each case is described in detail below. First, the syngas generation part is described, followed by the Low-Temperature FT (LT-FT) synthesis. The LT-FT process section remained the same for all cases since similar syngas throughput (in terms of H_2 and CO) was targeted to meet the

specification of an annual hydrocarbon production capacity of 222 kton. The syngas generation section was simulated in Aspen Plus. For the cases in which electrified heating was required, a heat transfer efficiency of 90% was applied, while a pressure drop value of 0.3 bar was assumed for the reactors, aligned with common practices found in the literature [59, 60]. In Fig. 1, the methodology is summarized.

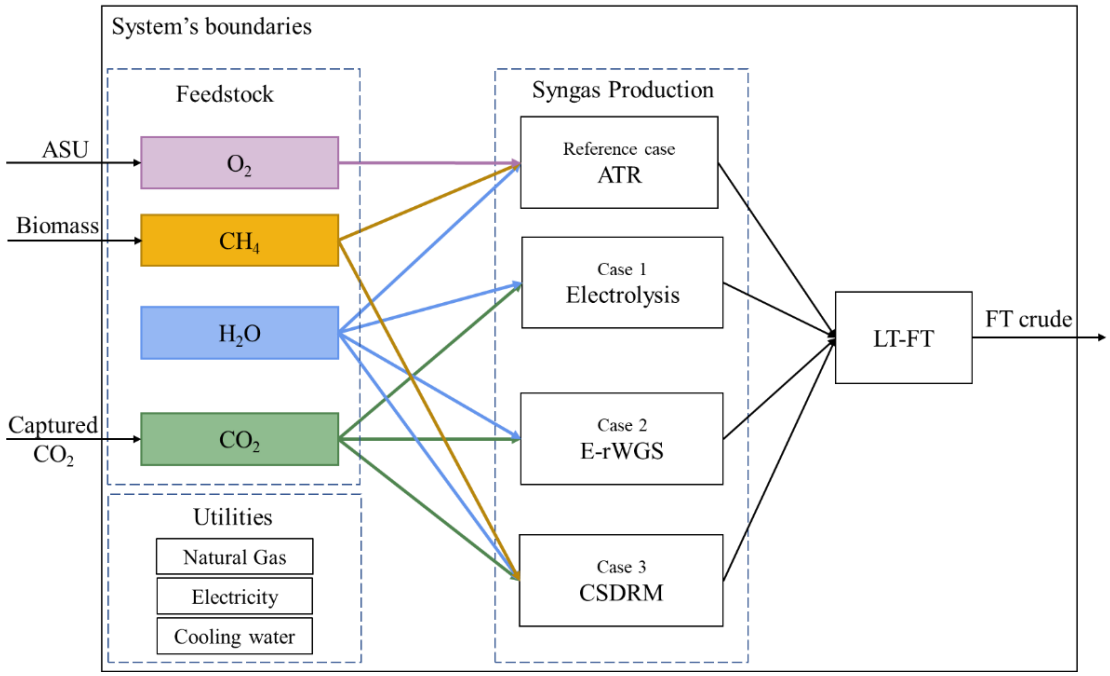

Fig. 1. System's boundaries and block flow diagram for the electrification of syngas production for the LT-FT process.

2.2.1. Reference case: ATR

The autothermal reforming technology is a combination of steam methane reforming and partial oxidation that requires steam, O_2, and CH_4 as feedstock, as described by the following reactions (R1-R9) [17].

$$CH_4 + H_2O \rightleftharpoons CO + 3H_2 \quad (\Delta H_{298} = 206.2 \text{ kJ/mol}) \qquad (R1)$$

$$CH_4 + 2H_2O \rightleftharpoons CO_2 + 4H_2 \quad (\Delta H_{298} = 164.9 \text{ kJ/mol}) \qquad (R2)$$

$$CO + H_2O \rightleftharpoons CO_2 + H_2 \quad (\Delta H_{298} = -41.1 \text{ kJ/mol}) \qquad (R3)$$

$$CH_4 + 2O_2 \rightleftharpoons CO_2 + 2H_2O \quad (\Delta H_{298} = -802.7 \text{ kJ/mol}) \qquad (R4)$$

$$CH_4 + \frac{1}{2}O_2 \rightleftharpoons CO + 2H_2 \quad (\Delta H_{298} = -36 \text{ kJ/mol}) \qquad (R5)$$

$$CH_4 + O_2 \rightleftharpoons CO_2 + 2H_2 \quad (\Delta H_{298} = -71 \text{ kJ/mol}) \qquad (R6)$$

$$CH_4 + CO_2 \rightleftharpoons 2CO + 2H_2 \quad (\Delta H_{298} = 247 \text{ kJ/mol}) \qquad (R7)$$

$$2CO \rightleftharpoons C + CO_2 \quad (\Delta H_{298} = -172 \text{ kJ/mol}) \qquad (R8)$$

$$CH_4 \rightleftharpoons C + 2H_2 \quad (\Delta H_{298} = 75 \text{ kJ/mol}) \qquad (R9)$$

The ATR reactor was simulated as a Gibbs reactor in Aspen Plus, where the Gibbs free energy is minimized so that the equilibrium compositions are calculated. The process flow diagram (PFD) is shown in Fig. 2. The reactor operated at a temperature of 1050 °C and pressure of 40 bar, utilizing a Ni-based catalyst. The process is exothermic, and therefore external cooling water was needed to maintain isothermal conditions. The mixture exiting the reactor was cooled down to 50 °C and sent into a flash to remove condensed water before it entered the FT reactor.

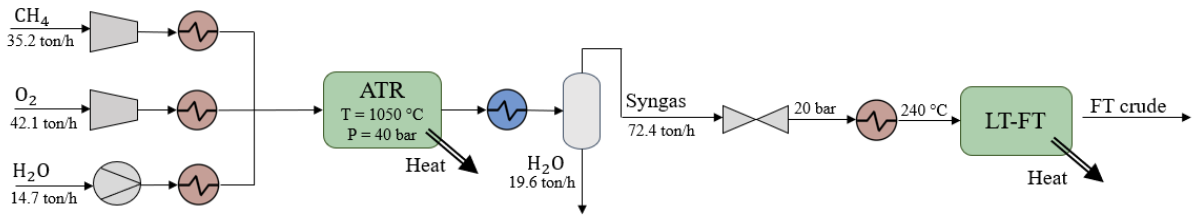

Fig. 2. Process flow diagram of the ATR case (Reference case).

2.2.2. Case 1: Electrolysis

Two separate electrolyzers were considered for the electrolysis of H_2O and the electrolysis of CO_2. For this system, the feedstock was H_2O and CO_2. The electrolyzers were simulated as black boxes. In the case of AWE, based on an equilibrium potential of 1.23 V [61] and a reported energy efficiency of 73% [62], the electricity consumption was calculated as 45.2 kWh/kg H_2. For the SOEC, based on an equilibrium potential of 1.34 V [63] and a lower energy efficiency of 40% due to the technology's early stages, the energy consumption was found equal to 6.4 kWh/kg CO.

The operating conditions and assumptions are summarized in Table 4, while the process flow diagram for the Electrolysis case is presented in Fig. 3. The generated syngas was cooled down to meet the FT reactor's operating conditions. The amount of O_2 that was produced in the electrolyzers was considered sold as a byproduct.

Table 4. Operating conditions and assumptions for the AWE and SOEC units.

Parameter	AWE	SOEC
Operating temperature (°C)	90	800
Operating pressure (bar)	20	20
Energy efficiency (%)	73	40
Electricity consumption	45.2 kWh/kg H_2	6.4 kWh/kg CO

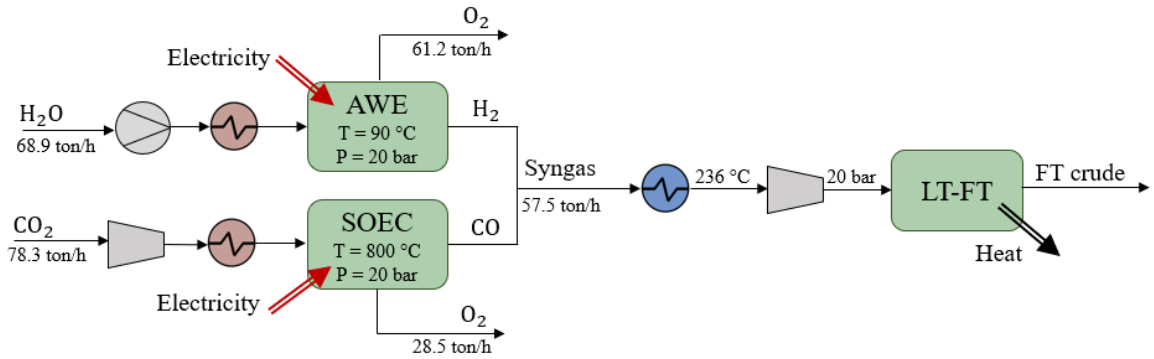

Fig. 3. Process flow diagram of the Electrolysis case.

2.2.3. Case 2: E-rWGS

The rWGS case required CO_2 and H_2, with the latter being derived from H_2O electrolysis, as described in the previous case. Therefore, the feedstock in this case was CO_2 and H_2O. The rWGS reaction is highly endothermic, and the reaction was conducted at 750 °C and 5 bar, implemented as an equilibrium reactor. The reactions that were considered are the rWGS reaction (R10) and the Sabatier reaction (R11) as the main side reaction.

$$CO_2 + H_2 \rightleftharpoons CO + H_2O \ (\Delta H_{298} = 41.1 \text{ kJ/mol}) \qquad \text{(R10)}$$

$$CO_2 + 4H_2 \rightleftharpoons CH_4 + 2H_2O \ (\Delta H_{298} = -165 \text{ kJ/mol}) \qquad \text{(R11)}$$

The reactor was assumed to be a multi-tubular fixed-bed reactor with a Ni-based catalyst; while the electrical heating was carried out by using resistive heating rods. The process flow diagram of this case is given in Fig. 4.

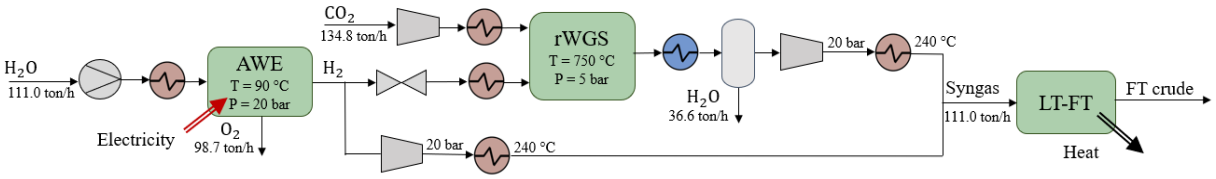

Fig. 4. Process flow diagram of the E-rWGS case.

2.2.4. Case 3: CSDRM

The most important reactions occurring are presented below and include the dry reforming (R12), the steam reforming (R13-R14), and the WGS (R15) reactions [64].

$$CH_4 + CO_2 \rightleftharpoons 2CO + 2H_2 \ (\Delta H_{298} = 247 \text{ kJ/mol}) \quad (R12)$$

$$CH_4 + H_2O \rightleftharpoons CO + 3H_2 \ (\Delta H_{298} = 206.2 \text{ kJ/mol}) \quad (R13)$$

$$CH_4 + 2H_2O \rightleftharpoons CO_2 + 4H_2 \ (\Delta H_{298} = 164.9 \text{ kJ/mol}) \quad (R14)$$

$$CO + H_2O \rightleftharpoons CO_2 + H_2 \ (\Delta H_{298} = -41.1 \text{ kJ/mol}) \quad (R15)$$

In this case the feedstock consisted of CH_4, H_2O, and CO_2, as shown in Fig. 5. The CSDRM operated at a temperature of 780 °C and pressure of 2.9 bar. A multi-tubular fixed bed reactor with a Ni-based catalyst was assumed, while the CSDRM reactor was implemented as an RGibbs reactor in Aspen Plus. The reactions occurring inside the CSDRM reactor are overall endothermic, so external, electrical heating was required to ensure isothermal conditions.

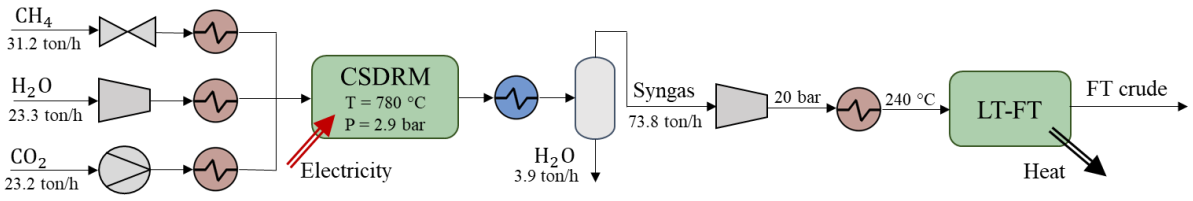

Fig. 5. Process flow diagram of the CSDRM case.

2.2.5. Fischer-Tropsch synthesis

FT is a widely investigated process. This study focuses on the LT-FT technology utilizing a Co-based catalyst which prohibits the occurrence of the WGS reaction. The LT-FT reactor was assumed to be an isothermal multi-tubular fixed-bed reactor that operates at 240 °C and 20 bar. The overall reaction (R16) is exothermic, and therefore external cooling was required.

$$CO + 2.15H_2 \rightarrow HCs + H_2O \ (\Delta H_{298} = -165 \text{ kJ/mol}) \quad (R16)$$

As stated before, the required syngas H_2:CO-ratio was set at 2.15 as a specification in the syngas production part for all cases. Additionally, in some of the cases, CO_2 and CH_4 were present in the syngas stream, resulting in different final syngas flow rates among the cases. More information about the composition of the syngas stream can be found in the Supplementary Information (SI). Nevertheless, as long as their concentration is less than 20 mol% and 10 mol% respectively, they can be considered diluents with a negligible impact on the production capacity [65, 66].

The distribution of the chain lengths of the produced hydrocarbons can be estimated by using the Anderson-Schulz-Flory (ASF) distribution, given by Eq. (1) [67].

$$W_n = n(1-\alpha)^2\alpha^{n-1} \quad (1)$$

W_n presents the weight fraction of the formed hydrocarbons with chain length n. The growth probability, α, can be estimated using the empirically determined correlations deduced by Song et al. [68] which depends on the H_2:CO-ratio and the operating temperature. The growth probability equals 0.762 for an LT-FT process at 240 °C, and an H_2:CO-ratio equal to 2.15 [68]. Table 5. presents the resulting

distribution of the formed hydrocarbons. It is concluded that most of the formed hydrocarbons are in the LPG-, light naphtha- and kerosene range. In practice, a fraction of the hydrocarbons are olefines; however, the amount is small and is further neglected in this study, where only paraffins were considered. Further information on the FT process can be found in the literature [13, 67].

Table 5. Product distribution of the formed hydrocarbons in the LT-FT synthesis.

Product	Methane	Ethane	LPG	Light naphtha	Kerosene	Waxes	Total
Mass fraction	0.06	0.09	0.20	0.26	0.34	0.06	1.00

3. Economic and environmental evaluation

3.1. Capital expenditure

The capital expenditure (CAPEX) was estimated prior to heat integration. To obtain a cost estimation for implementation, the sizing of equipment was performed based on correlations presented in the works of Guthrie [69] and Coulson and Richardson [70] unless mentioned otherwise. An update factor of 7.17 was used to account for the inflation between the studied (2022) and the reference year (1968). The installation costs were also included to obtain the inside battery limits (ISBL) costs using a module factor for each kind of equipment. The costs associated with offsites, engineering, and contingency were included by multiplying the ISBL with a factor of 1.82 to find the total fixed capital costs as reported in other studies and common methodologies [71, 72].

The cost associated with the first load of the catalysts was considered as capital cost, at a price of 16.0 $/kg for nickel- [73] and 23.5 $/kg for cobalt-based catalysts [74] respectively. For the electrolyzers, an investment cost of 865 $/kW was chosen based on the literature [75] and the assumption that the cost of the SOEC was the same as the AWE. As a wide range of electrolyzers' investment costs is provided in the literature, the value that was chosen is in the lower end, reflecting an optimistic perspective for the current study.

The CAPEX was then estimated by adding the working capital as 10% of the total fixed capital costs. More information about the detailed CAPEX estimation for each equipment can be found in the Supporting Information (SI).

3.2. Operational expenditure

The operational expenditure (OPEX) consists of a fixed and variable OPEX. The fixed annual OPEX includes the maintenance and personnel costs and was assumed to be 5% of the CAPEX. The variable OPEX was derived from the feedstock, utilities, and CO_2 tax for each case. Operational costs regarding the replacement of the catalysts were considered minor and were further neglected. The European trading system (ETS) CO_2 price in Europe has rapidly increased over the last years, therefore for the current study its price was considered equal to 88 $/ton of CO_2 produced [76].

3.3. Economic Analysis

To evaluate the commercial feasibility of each case, the Net Present Value (NPV) at the end of the project lifetime (i.e. after 20 years) was estimated, given by Eq. (2) for each year i:

$$\mathrm{NPV_i} = \mathrm{NPV_{i-1}} + \frac{\text{cash flow}_\mathrm{i}}{(1 + \text{discount rate})^\mathrm{i}} \qquad (2)$$

Where $\mathrm{NPV_0} = -\mathrm{CAPEX}$. A discount rate of 10% and a tax rate of 25% were taken into account.

The cash flow for each year i is given by Eq. (3)

$$\text{Cash flow}_\mathrm{i} = \mathrm{R_i} - \mathrm{OPEX_v} - \mathrm{OPEX_f} - \mathrm{T_i} \qquad (3)$$

Where R is the revenue, $\mathrm{OPEX_v}$ is the variable OPEX, $\mathrm{OPEX_f}$ is the fixed OPEX and $\mathrm{T_i}$ represents the taxes paid including the depreciation.

The levelized cost of production (LCOP) is a key performance indicator (KPI) that determines the economic viability of each process. This indicator was defined as the minimum value that the FT crude product can be sold so that the NPV is equal to \$0 after 20 years of the project's lifetime.

3.4. Environmental Analysis

An environmental evaluation was performed, accounting for direct and indirect CO_2 emissions related to each case. Net CO_2 emissions is a KPI that indicates the net environmental impact of the process in terms of emitted CO_2. This indicator accounted for (1) the sum of the CO_2 emissions, $\sum \mathrm{CO_{2,emitted}}$, caused by the electricity grid, heating via natural gas combustion, and the unreacted CO_2 amount in the syngas, and (2) the consumption of CO_2 as a feedstock, $\mathrm{CO_{2,consumed}}$, and is given by Eq. (4):

$$\text{Net } \mathrm{CO_2} \text{ emissions} = \sum \mathrm{CO_{2,emitted}} - \mathrm{CO_{2,consumed}} \qquad (4)$$

Negative values of net CO_2 emissions indicated that the process consumed more CO_2 than it emitted and was therefore overall net negative.

4. Results and Discussion

4.1. Energy demand

The results of the energy balance are shown in Fig. 6a. The Electrolysis case demonstrates a high demand for electricity for this capacity, reaching 673 MW. This substantial requirement is attributed to the AWE and SOEC units selected for syngas production, representing 51% and 47% of the total electricity consumption, respectively. Similarly, the E-rWGS case exhibits a significant electricity consumption of 585 MW, with AWE contributing to 96% of this demand. The CSDRM case presents a notably lower electricity need of 110 MW, mainly attributed to the electrified heating of the reactor. The ATR case shows a minimal electricity requirement of 2.9 MW, due to the autothermal nature of the ATR reactor. Following heat integration, the heating and cooling duties can be presented in Fig. 6b. The hot and cold composite graphs for each case can be found in the SI.

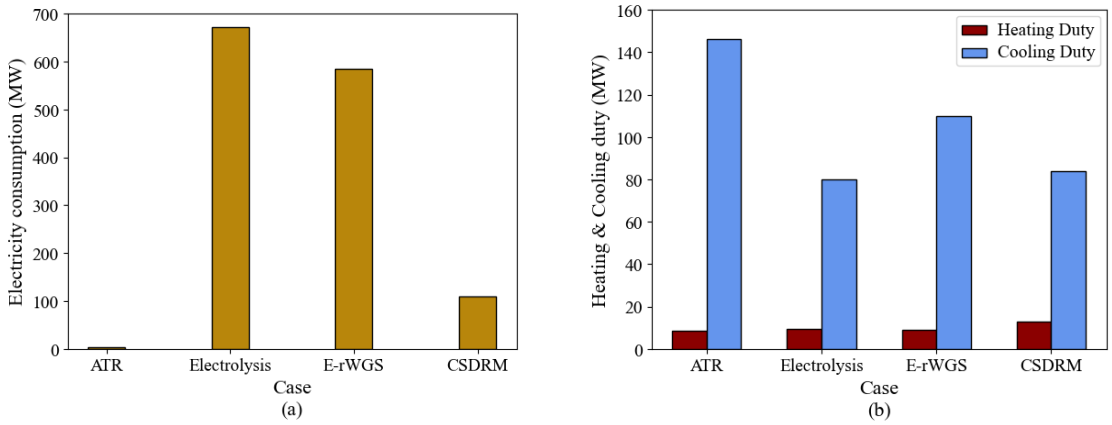

Fig. 6. (a) Electricity consumption and (b) residual heating and cooling duty after heat integration

4.2. Economic and Environmental Evaluation

The economic evaluation reveals a high CAPEX associated with the electrolyzers in the Electrolysis and E-rWGS cases (Fig. 7). The electrolyzers have an estimated investment cost (ISBL) of 865 $/kW. While this value currently reflects an optimistic perspective, it is justified due to the large scale of the unit while the technology will benefit from the economy of scale [77]. According to 2030 projections, AWE's direct cost could be expected to further drop at 420 €/kW (~47% reduction compared to the current study) due to technological improvements and optimizations [78]. This can reduce the CAPEX for both the Electrolysis and E-rWGS cases, bringing them closer to the Reference and CSDRM cases. The use of electrolyzers affects the operational costs as well, due to their high electricity demand. It should be noted that the electricity price chosen in this study, set at 113 $/MWh, is relatively high compared to other recent studies which typically report a value within the range of 40-80 $/MWh [71, 79, 80]. However, the selected value derives from a five-year average (2018-2022) for non-household EU power pricing, providing a realistic perspective [57]. Based on current estimations, both the Electrolysis and E-rWGS cases show large CAPEX and OPEX for such a large-scale system (>500 MW). Regarding the ATR (Reference) and the CSDRM case, a lower OPEX is reported, while the major costs are associated with the high biomethane price and consumption. The biomethane sector is expected to significantly evolve, particularly after the recent energy crisis [81]. Nevertheless, a long-term assessment of the profitability of biomethane production remains challenging due to the uncertainty related to its production cost [81].

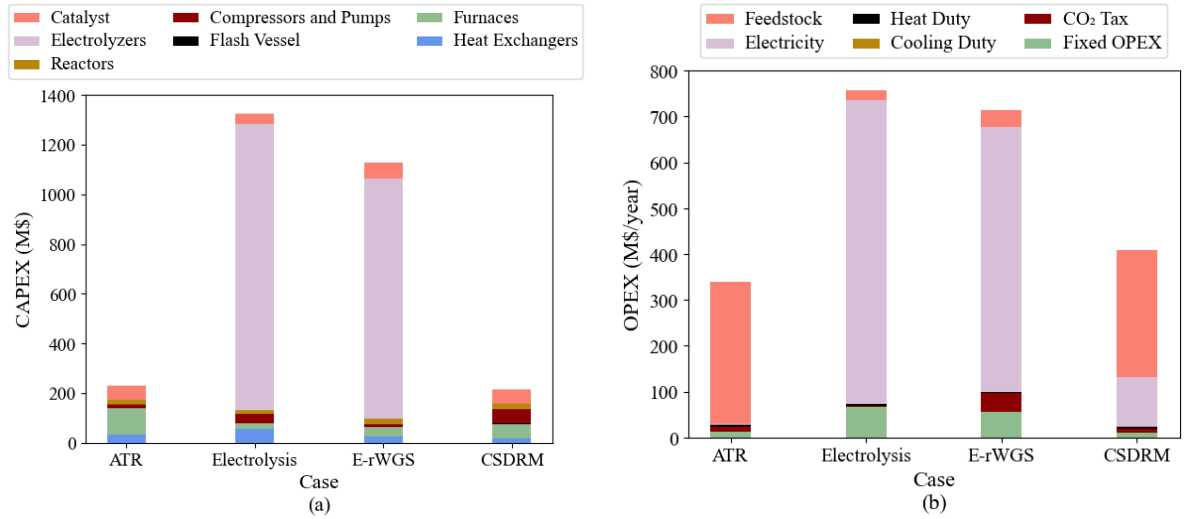

Fig. 7. (a) Breakdown of CAPEX and (b) Detailed breakdown of OPEX for all cases.

Fig. 8a illustrates the environmental impact analysis in terms of CO_2 emissions across all the cases. The CSDRM case shows the lowest net CO_2 emissions compared to all other cases, reaching 0.50 $ton_{CO2}/ton_{product}$. The ATR case also reports low emissions of 0.58 $ton_{CO2}/ton_{product}$, yet unavoidable since they originate from the CO_2 that is produced in the syngas section. Integration with Carbon Capture and Storage (CCS) technologies could mitigate these emissions [79], but increase the overall cost of the process. On the contrary, it is shown that the emissions related to the other three cases stem from the production of the electricity that is used in the processes. This shows the potential of all three cases to achieve net negative emissions if renewable electricity is used instead of electricity with the current grid average. Therefore, evaluating the impact of electricity emissions on the net CO_2 emissions is imperative, as depicted in Fig. 8b. The calculated data correspond to the base case (242 g_{CO2}/kWh), a 50% reduction (121 g_{CO2}/kWh), a 100% reduction (0 g_{CO2}/kWh), and a 50% increase (363 g_{CO2}/kWh) in the electricity emissions. The vertical dashed line indicates the EU's 2030 target for 40% overall renewable energy, according to which the electricity emissions would drop to 100 gCO_2/kWh. If this target is met, all the cases except for the ATR case would achieve net negative emissions. However, it should be noted that the chosen value for electricity emissions for the base case corresponds to an average EU level. Therefore, it does not uniformly represent all European countries, as for instance, on a 2018 basis, Sweden's emissions were 16 gCO_2/kWh, based on a hydro and nuclear network [82]. This highlights that net negative CO_2 emissions can be achievable under certain conditions.

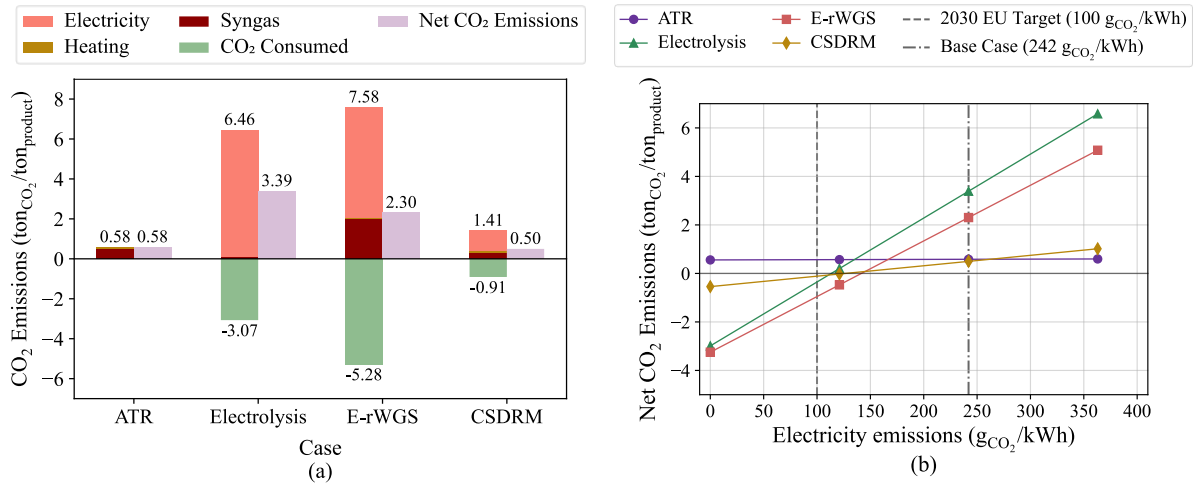

Fig. 8. (a) CO_2 emissions breakdown and (b) variation of the net CO_2 emissions with the electricity emissions for all cases.

4.3. Levelized Cost of Production and Sensitivity Analysis

Fig. 9 presents the LCOP for all the cases over a range of electricity prices considering an 80% reduction of the base case, i.e., an electricity price of 23 $/MWh up to a 20% increase, i.e., 136 $/MWh. A benchmark value of FT crude oil price of 69 $ per barrel (bbl) for the OPEC Basket oil from 2018 to 2022 is also included in the graph [83]. For the base case electricity price, i.e., 113 $/MWh, ATR shows the lowest LCOP equal to 229 $/bbl; nonetheless more than three times higher than the current benchmark price. The CSDRM case reports a slightly higher LCOP of 251 $/bbl. This value is competitive to the LCOP of the ATR (which serves as the reference case), demonstrating the potential of CSDRM as an alternative path for sustainable FT-crude production. On the other side, the E-rWGS and Electrolysis cases have a high LCOP, of 457 $/bbl and 501 $/bbl, respectively. These high values can be attributed to the elevated CAPEX of the electrolyzers and the high electricity demand (OPEX). Conducting a sensitivity analysis of the electricity price is crucial since the levelized cost of electricity (LCOE) of renewable energy sources fluctuates significantly among different kinds of sources [84, 85] and locations [86]. As an indicator, the LCOE of solar PV has dropped by 89% from 2010 to 2022 down to 49$/MWh, while onshore wind LCOE has dropped down to 33 $/MWh, both falling below the price of electricity obtained by the combustion of fossil fuels while being associated with much less CO_2 burden [87]. Regarding geographic considerations, the location chosen can affect the cost of the renewable electricity used and therefore significantly impact the OPEX of the process. Specifically, a favorable location can shift the LCOE by 50%, while also decreasing the uncertainty regarding this cost [86].

ATR shows minimal sensitivity to the electricity price and, therefore, the lowest potential for OPEX reduction. In contrast, the CSDRM case has the potential to reduce its LCOP to approximately 200 $/bbl at the lower end of the electricity cost range. Both the E-rWGS and Electrolysis cases show significant

potential for cost reduction, achieving an LCOP below 200 $/bbl with an 80% reduction in electricity price. However, even at an 80% reduction in electricity price, all cases demonstrate a ~3 times higher LCOP compared to the benchmark price, albeit still lower than ATR's LCOP. The revenues of all cases derive from selling the FT crude product. In addition, for the Electrolysis and E-rWGS cases, extra revenue is taken into account by considering that the O_2 produced is also sold as a by-product. For the base case, this additional O_2 sell reduces the LCOP of the Electrolysis and E-rWGS cases by 7.4% and 8.84%, respectively.

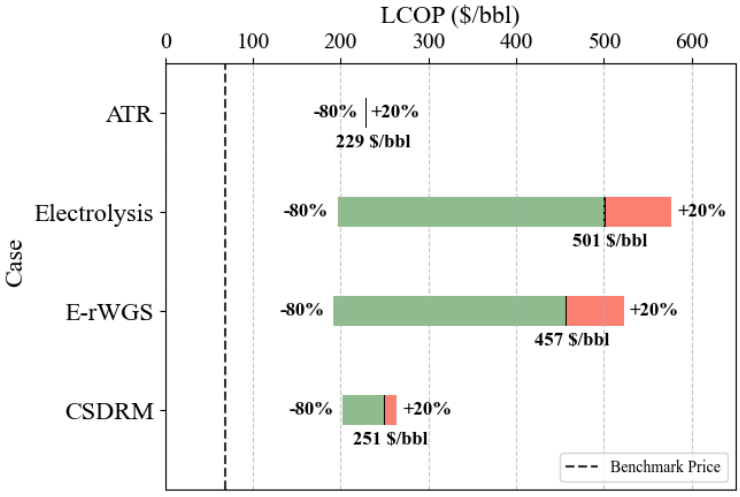

Fig. 9. Levelized cost of production (LCOP) of all cases over a range of electricity prices (-80%, base case, +20%).

As the different cases show a variance in cost drivers, a sensitivity graph (Fig. 10) has been constructed to evaluate the economic viability of each case under different scenarios. These scenarios have been selected based on optimistic prospects and future projections regarding the cost drivers of the processes. The main cost driver of the ATR and the CSDRM cases is the biomethane price. Therefore, two scenarios have been studied for each case, i.e., a 20% and a 40% reduction in biomethane price. Notably, at a 40% reduction in biomethane price, the price aligns with the reference natural gas price in this study. Regarding the Electrolysis and the E-rWGS cases, a main cost driver is the CAPEX of the electrolyzers. The two scenarios chosen for each of these cases correspond to a 25% and 50% reduction of the electrolyzers' CAPEX. At 50% electrolyzers CAPEX decrease, the CAPEX approaches the previously reported value of the 2030 projection [78]. The LCOP of all scenarios is reported over the same electricity price range as in Fig. 9, i.e. considering the base case (electricity price of 113 $/MWh), an 80% reduction (23 $/MWh), and a 20% increase (136 $/MWh). The CSDRM case appears to have a stronger sensitivity to the electricity price compared to the ATR case, which is only affected by the biomethane price. Within the specific biomethane price values, the CSDRM case emerges as more economically feasible than the ATR case when the electricity price drops around 40%, reaching a value of approximately 60-70 $/MWh. Under the most optimistic scenario for CSDRM in terms of both

biomethane price (40% reduction) and electricity price (80% reduction), the LCOP is twice as high as the benchmark price.

A similar conclusion can be drawn for the Electrolysis and E-rWGS cases. These cases showcase a heightened sensitivity to electricity prices due to the use of electrolyzers. However, for an 80% reduction in the electricity price, they reach the same level of LCOP as the CSDRM's case. The E-rWGS case appears to constantly have a lower LCOP than the Electrolysis case for the base case of electricity price. However, under the most optimistic scenario in terms of electrolyzers' CAPEX (50% reduction) and electricity price (80% reduction), the Electrolysis case shows the lowest LCOP reported within the chosen economic parameters, reaching 134 $/bbl. Utilizing the dataset depicting a 50% reduction in electrolyzer CAPEX we extrapolate the electricity price necessary to achieve the benchmark price (highlighted in the graph by red dashed lines). Economic feasibility for the Electrolysis case is attained when the electricity price falls below 3.3 $/MWh.

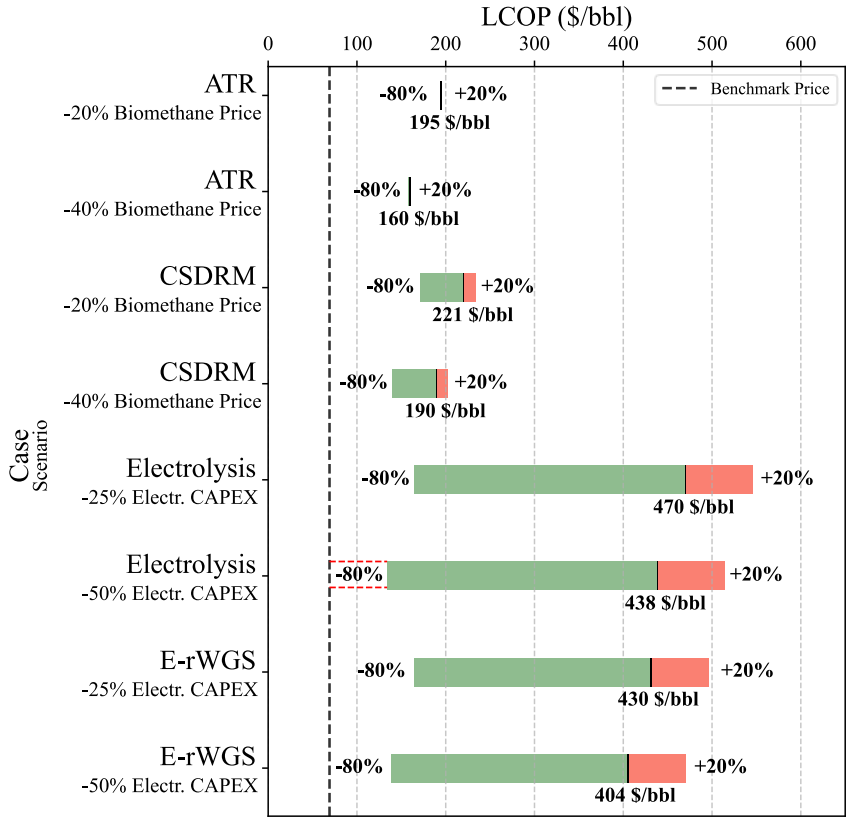

Fig. 10. Variation of the levelized cost of production (LCOP) of all cases over a range of electricity prices (-80%, base case, +20%) under various scenarios.

A SWOT (Strengths, Weaknesses, Opportunities, Threats) analysis is performed (Table 6), summarizing the findings of this study. The ATR case shows high stability in terms of emissions, while its economics are strongly affected by the biomethane price. The calculated LCOP is the lowest among all cases, at 229 $/bbl. However, this case does not show any potential benefits for electrification transition or major cost reductions. One interesting approach to reducing the emissions associated with ATR technologies

would be coupling the process with CCS technologies. Nonetheless, such venture would increase the LCOP of the process. Notably, a considerable weakness of autothermal reforming is the need for pure O_2 [11]. ASU can be an energy-intensive process [88] that should be taken into account in a comprehensive life cycle assessment (LCA) that initiates from raw materials. In this study, the CO_2 emissions from the ASU were not considered. An alternative approach could include a water electrolyzer to provide the required O_2 through a hybrid process that couples the ATR technology with electrolysis while producing an excess amount of H_2 [89].

The three electrified cases showcase a high potential for negative emissions, as well as a high sensitivity to their respective cost drivers. CSDRM appears to be the most promising option under the current circumstances. It has the lowest LCOP (251 $/bbl) and the lowest net CO_2 emissions (0.50 $ton_{CO2}/ton_{product}$) while being sensitive to the electricity price. On the downside, it has a high dependency on biomethane, whose future is yet unpredictable. Although the Electrolysis and E-rWGS scenarios currently lag behind in terms of economic viability and environmental impact, future trends suggest a shift in their favor. Anticipated advancements in renewable energy production and the scaling-up of electrolyzers are poised to enhance the competitiveness of these processes relative to the CSDRM case. Given sufficiently low electricity prices, the Electrolysis scenario could even approach the current benchmark price. However, it is important to acknowledge that none of the electrified scenarios currently exhibit a significant edge in terms of economic feasibility. Future progress in scaling up electrolyzers, increasing the supply of renewable energy, expanding biomethane production, and innovating catalysts will play a pivotal role in determining which scenario, if any, emerges as a standout option. As access to green electricity expands and carbon capture technologies rapidly evolve, prudent consideration of these alternative resources becomes increasingly imperative.

Table 6. SWOT analysis with strengths, weaknesses, opportunities, and threats of the selected cases for the electrification of syngas production.

	Strengths	Weaknesses	Opportunities	Threats
ATR	➢ Mature Technology ➢ Low LCOP ➢ Low carbon footprint compared to SMR	➢ Not suitable for electrification transition ➢ Need for O_2	➢ Biomethane sector acceleration ➢ Coupling with CCS ➢ Coupling with water electrolysis	➢ Unpredictable biomethane price
Electrolysis	➢ Good integration with electrification transition ➢ Low/Negative net CO_2 emissions ➢ High purity syngas ➢ Cost-competitive in future projections ➢ Upgrade CO_2 from CCU	➢ High LCOP ➢ High dependency on electricity price and energy source ➢ Low durability of electrolyzers ➢ Small scale electrolyzers	➢ Increasing availability of renewable energy ➢ Carbon circularity ➢ Increasing availability of CCS	➢ Need for electrolyzers scale-up and CAPEX reduction ➢ Further research is needed on CO_2 electrolyzers

E-rWGS	➢ Good integration with electrification transition ➢ Low/Negative net CO_2 emissions ➢ Upgrade CO_2 from CCU		➢ Technological development of electrolyzers	➢ Further research is needed on catalyst development ➢ Need for electrolyzers scale-up and CAPEX reduction
CSDRM	➢ Lowest LCOP among electrified cases ➢ Low/Negative net CO_2 emissions ➢ Upgrade CO_2 from CCU	➢ Dependency on biomethane	➢ Biomethane sector acceleration ➢ Carbon circularity ➢ Increasing availability of CCS	➢ Unpredictable biomethane price ➢ Further research on catalyst development

5. Conclusions

Three distinct pathways for electrified and sustainable syngas production, integrated with low-temperature Fischer-Tropsch synthesis for generating 222 kton of FT crude annually, were investigated. An exhaustive energy assessment preceded a high-level evaluation of techno-economic factors and GHG emissions impact.

In the first scenario, termed "Electrolysis," electrolyzers were solely utilized to produce syngas, resulting in an LCOP of 501 \$/bbl and net CO_2 emissions of 3.39 $ton_{CO2}/ton_{product}$, based on current electricity grid data. The second scenario, "E-rGWS," combined a water electrolyzer with the reverse water-gas shift reaction, showcasing an LCOP of 457 \$/bbl and net CO_2 emissions of 2.30 $ton_{CO2}/ton_{product}$. These cases incurred excessive costs attributed to the substantial CAPEX of the electrolyzers and elevated electricity demands leading to increased OPEX.

The third scenario, "CSDRM," entailed combined steam and dry reforming of biomethane, boasting the lowest LCOP at 251 \$/bbl and the least net CO_2 emissions of 0.50 $ton_{CO2}/ton_{product}$, emerging as the most promising option presently. Additionally, the autothermal reforming of biomethane (ATR) served as a reference case, yielding an LCOP of 229 \$/bbl and net CO_2 emissions of 0.58 $ton_{CO2}/ton_{product}$.

The techno-economic analysis revealed that the feasibility of the CSDRM case surpasses the reference case when electricity prices drop below 60-70 \$/MWh. However, its LCOP remains higher than the benchmark due to biomethane's costly nature. Nevertheless, future trends indicating the commercialization and cost reduction of electrolyzers could enhance the viability of other electrified cases. Projections suggest that the Electrolysis and E-rGWS cases could compete with the reference case, especially if electricity prices plummet to 3.3 \$/MWh. Such prices, albeit unrealistic currently, hinge on substantial advancements or potential price increases of the benchmark product.

A sensitivity analysis underscored the potential of electrified cases across various scenarios. From a CO_2-emission standpoint, achieving the EU target of 40% overall renewable energy production by 2030

would render all three electrified cases net-negative in CO_2 emissions, with the E-rWGS case exhibiting the most significant decrease.

The feasibility of electrified processes hinges on several distinct factors. Technological advancements, particularly in cell stack development for electrolyzers and catalysts for rWGS and CSDRM, are paramount. Globally, increased availability and reduced costs of renewable energy and biomethane production capacity are vital. Political support, in the form of rewarding ETS regulations rather than burdensome CO_2 emission taxes, is imperative for transitioning to electrified, net-zero, or net-negative emission technologies.

CRediT author statement

Afroditi Kourou: Methodology, Investigation, Writing - Original Draft **Simon De Langhe:** Investigation, Writing - Original Draft **Lander Nelis:** Investigation, Writing - Original Draft **Yannick Ureel:** Conceptualization, Methodology, Writing - Review & Editing **Matthijs Ruitenbeek:** Supervision, Conceptualization, Writing - Review & Editing **Kees Biesheuvel:** Conceptualization, Methodology **Ronald Wevers:** Conceptualization, Methodology **Yi Ouyang:** Supervision, Writing - Review & Editing **Kevin M. Van Geem:** Supervision, Project administration, Funding acquisition, Writing - Review & Editing

Acknowledgment

This research is part of the MuSE project, which is a Belgian academic collaboration project, funded by the federal Energy Transition Fund by FPS Economy. More information on www.molecules-at-sea.eu. Yannick Ureel acknowledges financial support from the Fund for Scientific Research Flanders (FWO Flanders) through the doctoral fellowship grant 1185822N. The research leading to these results has received funding from the European Research Council under the European Union's Horizon 2020 research and innovation programme / ERC grant agreement n° 818607.

References

[1] H. Wiertzema, E. Svensson, S. Harvey, Bottom–up assessment framework for electrification options in energy-intensive process industries, Frontiers in Energy Research 8 (2020) 192. https://doi.org/10.3389/fenrg.2020.00192.

[2] J. Tickner, K. Geiser, S. Baima, Transitioning the chemical industry: the case for addressing the climate, toxics, and plastics crises, Environment: Science and Policy for Sustainable Development 63(6) (2021) 4-15. https://doi.org/10.1080/00139157.2021.1979857.

[3] E. Meloni, Electrification of Chemical Engineering: A New Way to Intensify Chemical Processes, MDPI, 2022, p. 5469.

[4] J. Rissman, C. Bataille, E. Masanet, N. Aden, W.R. Morrow III, N. Zhou, N. Elliott, R. Dell, N. Heeren, B. Huckestein, Technologies and policies to decarbonize global industry: Review and assessment of mitigation drivers through 2070, Applied energy 266 (2020) 114848. https://doi.org/10.1016/j.apenergy.2020.114848.

[5] G. Lagioia, M.P. Spinelli, V. Amicarelli, Blue and green hydrogen energy to meet European Union decarbonisation objectives. An overview of perspectives and the current state of affairs, International Journal of Hydrogen Energy 48(4) (2023) 1304-1322. https://doi.org/https://doi.org/10.1016/j.ijhydene.2022.10.044.
[6] M. Wei, C.A. McMillan, S. de la Rue du Can, Electrification of industry: Potential, challenges and outlook, Current Sustainable/Renewable Energy Reports 6 (2019) 140-148.
[7] Z.J. Schiffer, K. Manthiram, Electrification and Decarbonization of the Chemical Industry, Joule 1(1) (2017) 10-14. https://doi.org/https://doi.org/10.1016/j.joule.2017.07.008.
[8] C.A.R. Pappijn, M. Ruitenbeek, M.-F. Reyniers, K.M. Van Geem, Challenges and Opportunities of Carbon Capture and Utilization: Electrochemical Conversion of CO2 to Ethylene, Frontiers in Energy Research 8 (2020). https://doi.org/10.3389/fenrg.2020.557466.
[9] P. Buchenberg, T. Addanki, D. Franzmann, C. Winkler, F. Lippkau, T. Hamacher, P. Kuhn, H. Heinrichs, M. Blesl, Global potentials and costs of synfuels via Fischer–Tropsch process, Energies 16(4) (2023) 1976. https://doi.org/10.3390/en16041976.
[10] M.P. Jones, T. Krexner, A. Bismarck, Repurposing Fischer-Tropsch and natural gas as bridging technologies for the energy revolution, Energy Conversion and Management 267 (2022) 115882. https://doi.org/10.1016/j.enconman.2022.115882.
[11] R. Kumar, A. Kumar, A. Pal, Overview of hydrogen production from biogas reforming: Technological advancement, International Journal of Hydrogen Energy 47(82) (2022) 34831-34855. https://doi.org/https://doi.org/10.1016/j.ijhydene.2022.08.059.
[12] IEA, Outlook for biogas and biomethane, Prospects for organic growth World Energy Outlook Special Report, 2020.
[13] M. Martinelli, M.K. Gnanamani, S. LeViness, G. Jacobs, W.D. Shafer, An overview of Fischer-Tropsch Synthesis: XtL processes, catalysts and reactors, Applied Catalysis A: General 608 (2020) 117740. https://doi.org/10.1016/j.apcata.2020.117740.
[14] P. Kiani, H.R. Rahimpour, M.R. Rahimpour, Chapter 4 - Steam reforming process for syngas production, in: M.R. Rahimpour, M.A. Makarem, M. Meshksar (Eds.), Advances in Synthesis Gas : Methods, Technologies and Applications, Elsevier2023, pp. 81-96. https://doi.org/https://doi.org/10.1016/B978-0-323-91871-8.00001-5.
[15] P. Sun, B. Young, A. Elgowainy, Z. Lu, M. Wang, B. Morelli, T. Hawkins, Criteria air pollutants and greenhouse gas emissions from hydrogen production in US steam methane reforming facilities, Environmental science & technology 53(12) (2019) 7103-7113. https://doi.org/10.1021/acs.est.8b06197.
[16] P. Nikolaidis, A. Poullikkas, A comparative overview of hydrogen production processes, Renewable and sustainable energy reviews 67 (2017) 597-611. https://doi.org/10.1016/j.rser.2016.09.044.
[17] M. Halabi, M. De Croon, J. Van der Schaaf, P. Cobden, J. Schouten, Modeling and analysis of autothermal reforming of methane to hydrogen in a fixed bed reformer, Chemical Engineering Journal 137(3) (2008) 568-578. https://doi.org/10.1016/j.cej.2007.05.019.
[18] T.L. de Souza, C.d.C.R.d.S. Rossi, C.G. Alonso, R. Guirardello, V.F. Cabral, N.R.C. Fernandes-Machado, S. Specchia, M.S. Zabaloy, L. Cardozo-Filho, Thermodynamic analysis of autothermal reforming of methane via entropy maximization: Hydrogen production, International Journal of Hydrogen Energy 39(16) (2014) 8257-8270. https://doi.org/https://doi.org/10.1016/j.ijhydene.2014.03.078.
[19] S.F. Rice, D.P. Mann, Autothermal reforming of natural gas to synthesis gas, Sandia National Laboratories (SNL), Albuquerque, NM, and Livermore, CA, 2007.
[20] C. Antonini, K. Treyer, A. Streb, M. van der Spek, C. Bauer, M. Mazzotti, Hydrogen production from natural gas and biomethane with carbon capture and storage–A techno-environmental analysis, Sustainable Energy & Fuels 4(6) (2020) 2967-2986.
[21] U. Ahmed, M.A. Hussain, M. Bilal, H. Zeb, N. Ahmad, N. Ahmad, M. Usman, Production of hydrogen from low rank coal using process integration framework between syngas production processes: techno-economic analysis, Chemical Engineering and Processing-Process Intensification 169 (2021) 108639.

[22] IEA, Global Hydrogen Review 2022 – Analysis, 2022.
[23] P. Afanasev, A. Askarova, T. Alekhina, E. Popov, S. Markovic, A. Mukhametdinova, A. Cheremisin, E. Mukhina, An overview of hydrogen production methods: Focus on hydrocarbon feedstock, International Journal of Hydrogen Energy 78 (2024) 805-828. https://doi.org/https://doi.org/10.1016/j.ijhydene.2024.06.369.
[24] A. Mio, E. Barbera, A. Massi Pavan, A. Bertucco, M. Fermeglia, Sustainability analysis of hydrogen production processes, International Journal of Hydrogen Energy 54 (2024) 540-553. https://doi.org/https://doi.org/10.1016/j.ijhydene.2023.06.122.
[25] Q. Hassan, A.Z. Sameen, H.M. Salman, M. Jaszczur, Large-scale green hydrogen production via alkaline water electrolysis using solar and wind energy, International Journal of Hydrogen Energy 48(88) (2023) 34299-34315. https://doi.org/https://doi.org/10.1016/j.ijhydene.2023.05.126.
[26] S. Grigoriev, V. Fateev, D. Bessarabov, P. Millet, Current status, research trends, and challenges in water electrolysis science and technology, International Journal of Hydrogen Energy 45(49) (2020) 26036-26058. https://doi.org/10.1016/j.ijhydene.2020.03.109.
[27] A. Ursúa Rubio, L. Gandía Pascual, P. Sanchis Gúrpide, Hydrogen production from water electrolysis: current status and future trends, Proceedings of the IEEE, 100 (2), 2012 (2012).
[28] M. Rashid, M.K. Al Mesfer, H. Naseem, M. Danish, Hydrogen production by water electrolysis: a review of alkaline water electrolysis, PEM water electrolysis and high temperature water electrolysis, International Journal of Engineering and Advanced Technology (2015).
[29] Q. Hassan, S. Algburi, A.Z. Sameen, H.M. Salman, M. Jaszczur, Green hydrogen: A pathway to a sustainable energy future, International Journal of Hydrogen Energy 50 (2024) 310-333. https://doi.org/https://doi.org/10.1016/j.ijhydene.2023.08.321.
[30] A.Z. Arsad, M.A. Hannan, A.Q. Al-Shetwi, M.J. Hossain, R.A. Begum, P.J. Ker, F. Salehi, K.M. Muttaqi, Hydrogen electrolyser for sustainable energy production: A bibliometric analysis and future directions, International Journal of Hydrogen Energy 48(13) (2023) 4960-4983. https://doi.org/https://doi.org/10.1016/j.ijhydene.2022.11.023.
[31] C. Coutanceau, S. Baranton, T. Audichon, Hydrogen Production from Water Electrolysis, Hydrogen Electrochemical Production, Elsevier, Amsterdam, the Netherland, 2018.
[32] F. Rahim Malik, H.-B. Yuan, J.C. Moran, N. Tippayawong, Overview of hydrogen production technologies for fuel cell utilization, Engineering Science and Technology, an International Journal 43 (2023) 101452. https://doi.org/https://doi.org/10.1016/j.jestch.2023.101452.
[33] N.J. Rubinsin, N.A. Karim, S.N. Timmiati, K.L. Lim, W.N.R.W. Isahak, M. Pudukudy, An overview of the enhanced biomass gasification for hydrogen production, International Journal of Hydrogen Energy 49 (2024) 1139-1164. https://doi.org/https://doi.org/10.1016/j.ijhydene.2023.09.043.
[34] I. Inamuddin, A.M. Asiri, E. Lichtfouse, Conversion of Carbon Dioxide into Hydrocarbons Vol. 1 Catalysis, Springer Nature2020.
[35] M. Zhu, Q. Ge, X. Zhu, Catalytic reduction of CO 2 to CO via reverse water gas shift reaction: Recent advances in the design of active and selective supported metal catalysts, Transactions of Tianjin University 26 (2020) 172-187.
[36] R.M. Bown, M. Joyce, Q. Zhang, T.R. Reina, M.S. Duyar, Identifying commercial opportunities for the reverse water gas shift reaction, Energy Technology 9(11) (2021) 2100554. https://doi.org/10.1002/ente.202100554.
[37] Q. Zhang, L. Pastor-Pérez, W. Jin, S. Gu, T.R. Reina, Understanding the promoter effect of Cu and Cs over highly effective β-Mo2C catalysts for the reverse water-gas shift reaction, Applied Catalysis B: Environmental 244 (2019) 889-898. https://doi.org/10.1016/j.apcatb.2018.12.023.
[38] Q. Zhang, L. Pastor-Pérez, S. Gu, T. Ramirez Reina, Transition metal carbides (TMCS) catalysts for gas phase CO2 upgrading reactions: A comprehensive overview, Catalysts 10(9) (2020) 955.
[39] N. Farrell, Policy design for green hydrogen, Renewable and Sustainable Energy Reviews 178 (2023) 113216. https://doi.org/https://doi.org/10.1016/j.rser.2023.113216.
[40] W. Zhang, Y. Hu, L. Ma, G. Zhu, Y. Wang, X. Xue, R. Chen, S. Yang, Z. Jin, Progress and Perspective of Electrocatalytic CO2 Reduction for Renewable Carbonaceous Fuels and Chemicals, Advanced Science 5(1) (2018) 1700275. https://doi.org/https://doi.org/10.1002/advs.201700275.

[41] X. Du, P. Zhang, G. Zhang, H. Gao, L. Zhang, M. Zhang, T. Wang, J. Gong, Confinement of ionomer for electrocatalytic CO2 reduction reaction via efficient mass transfer pathways, National Science Review 11(2) (2023). https://doi.org/10.1093/nsr/nwad149.
[42] S. Jin, Z. Hao, K. Zhang, Z. Yan, J. Chen, Advances and Challenges for the Electrochemical Reduction of CO2 to CO: From Fundamentals to Industrialization, Angewandte Chemie International Edition 60(38) (2021) 20627-20648. https://doi.org/10.1002/anie.202101818.
[43] R. Küngas, electrochemical CO2 reduction for CO production: comparison of low-and high-temperature electrolysis technologies, Journal of The Electrochemical Society 167(4) (2020) 044508.
[44] J. Nørskov, B. Weckhuysen, G. Centi, S.R. ChorkendorffI, G. Marin, A. Grimaud, J. Rossmeisl, P. Strasser, M. Koper, B. Roldan, Research needs towards sustainable production of fuels and chemicals, Energy X (2019).
[45] B. Endrodi, E. Kecsenovity, A. Samu, F. Darvas, R. Jones, V. Torok, A. Danyi, C. Janáky, Multilayer electrolyzer stack converts carbon dioxide to gas products at high pressure with high efficiency, ACS energy letters 4(7) (2019) 1770-1777. https://doi.org/10.1021/acsenergylett.9b01142.
[46] A. Abdulrasheed, A.A. Jalil, Y. Gambo, M. Ibrahim, H.U. Hambali, M.Y.S. Hamid, A review on catalyst development for dry reforming of methane to syngas: Recent advances, Renewable and Sustainable Energy Reviews 108 (2019) 175-193. https://doi.org/10.1016/j.rser.2019.03.054.
[47] A.M. Ranjekar, G.D. Yadav, Dry reforming of methane for syngas production: A review and assessment of catalyst development and efficacy, Journal of the Indian Chemical Society 98(1) (2021) 100002. https://doi.org/10.1016/j.jics.2021.100002.
[48] D.P. Minh, T.J. Siang, D.-V.N. Vo, T.S. Phan, C. Ridart, A. Nzihou, D. Grouset, Hydrogen production from biogas reforming: an overview of steam reforming, dry reforming, dual reforming, and tri-reforming of methane, Hydrogen supply chains (2018) 111-166.
[49] N. Schiaroli, M. Volanti, A. Crimaldi, F. Passarini, A. Vaccari, G. Fornasari, S. Copelli, F. Florit, C. Lucarelli, Biogas to syngas through the combined steam/dry reforming process: an environmental impact assessment, Energy & Fuels 35(5) (2021) 4224-4236. https://doi.org/10.1021/acs.energyfuels.0c04066.
[50] Y. Lim, C.-J. Lee, Y.S. Jeong, I.H. Song, C.J. Lee, C. Han, Optimal design and decision for combined steam reforming process with dry methane reforming to reuse CO2 as a raw material, Industrial & engineering chemistry research 51(13) (2012) 4982-4989. https://doi.org/10.1021/ie200870m.
[51] D. Demidov, I. Mishin, M. Mikhailov, Gibbs free energy minimization as a way to optimize the combined steam and carbon dioxide reforming of methane, International Journal of Hydrogen Energy 36(10) (2011) 5941-5950. https://doi.org/10.1016/j.ijhydene.2011.02.053.
[52] K. Jabbour, Tuning combined steam and dry reforming of methane for “metgas” production: A thermodynamic approach and state-of-the-art catalysts, Journal of Energy Chemistry 48 (2020) 54-91. https://doi.org/10.1016/j.jechem.2019.12.017.
[53] S. Brown, D. Jones, Europian Electricity Review 2024, 2024.
[54] J.M. Moch, W. Xue, J.P. Holdren, Carbon capture, utilization, and storage: technologies and costs in the US context, Harvard Kennedy School Belfer Center Policy Brief (2022).
[55] Intratec Solutions LLC, Oxygen Price | Industrial Utilities. https://www.intratec.us/products/water-utility-costs/commodity/oxygen-price. (Accessed 10/01/2024.
[56] I.C. Kemp, J.S. Lim, Pinch Analysis for Energy and Carbon Footprint Reduction, Batch and time-dependent processes (2020) 317-349.
[57] Electricity prices for non-household consumers - bi-annual data (from 2007 onwards). https://ec.europa.eu/eurostat/databrowser/view/nrg_pc_205/default/line?lang=en. (Accessed 30/06/2023.
[58] Gas prices for non-household consumers - bi-annual data (from 2007 onwards). https://ec.europa.eu/eurostat/databrowser/view/NRG_PC_203/default/table?lang=en&category=nrg.nrg_price.nrg_pc. (Accessed 30/06/2023.

[59] A. Mion, F. Galli, P. Mocellin, S. Guffanti, G. Pauletto, Electrified methane reforming decarbonises methanol synthesis, Journal of CO2 Utilization 58 (2022) 101911. https://doi.org/https://doi.org/10.1016/j.jcou.2022.101911.
[60] M.E. Diego, J.C. Abanades, Techno-economic analysis of a low carbon back-up power system using chemical looping, Renewable and Sustainable Energy Reviews 132 (2020) 110099. https://doi.org/https://doi.org/10.1016/j.rser.2020.110099.
[61] Ø. Ulleberg, Modeling of advanced alkaline electrolyzers: a system simulation approach, International journal of hydrogen energy 28(1) (2003) 21-33. https://doi.org/10.1016/S0360-3199(02)00033-2.
[62] F. Gambou, D. Guilbert, M. Zasadzinski, H. Rafaralahy, A Comprehensive Survey of Alkaline Electrolyzer Modeling: Electrical Domain and Specific Electrolyte Conductivity, Energies 15(9) (2022) 3452. https://doi.org/10.3390/en15093452.
[63] Y. Wang, J. Liu, Y. Wang, A.M. Al-Enizi, G. Zheng, Tuning of CO2 reduction selectivity on metal electrocatalysts, Small 13(43) (2017) 1701809. https://doi.org/10.1002/smll.201701809.
[64] M. Dan, M. Mihet, M.D. Lazar, Hydrogen and/or syngas production by combined steam and dry reforming of methane on nickel catalysts, International Journal of Hydrogen Energy 45(49) (2020) 26254-26264.
[65] M.K. Gnanamani, W.D. Shafer, D.E. Sparks, B.H. Davis, Fischer–Tropsch synthesis: Effect of CO2 containing syngas over Pt promoted Co/γ-Al2O3 and K-promoted Fe catalysts, Catalysis Communications 12(11) (2011) 936-939. https://doi.org/10.1016/j.catcom.2011.03.002.
[66] M.E. Dry, The Fischer–Tropsch process: 1950–2000, Catalysis Today 71(3) (2002) 227-241. https://doi.org/https://doi.org/10.1016/S0920-5861(01)00453-9.
[67] S. Saeidi, M.K. Nikoo, A. Mirvakili, S. Bahrani, N.A.S. Amin, M.R. Rahimpour, Recent advances in reactors for low-temperature Fischer-Tropsch synthesis: process intensification perspective, Reviews in Chemical Engineering 31(3) (2015) 209-238. https://doi.org/doi:10.1515/revce-2014-0042.
[68] H.-S. Song, D. Ramkrishna, S. Trinh, H. Wright, Operating strategies for Fischer-Tropsch reactors: A model-directed study, Korean Journal of Chemical Engineering 21(2) (2004) 308-317. https://doi.org/10.1007/BF02705414.
[69] K.M. Guthrie, Process plant estimating, evaluation, and control, Craftsman Book Co. of America Los Angeles, Los Angeles, 1974.
[70] R.K. Sinnott, J.M. Coulson, J.F. Richardson, Coulson & Richardson's chemical engineering. Vol. 6, Chemical engineering design, Elsevier Butterworth-Heinemann Oxford, Oxford, 2005.
[71] L. Berkelaar, J. van der Linde, J. Peper, A. Rajhans, D. Tiemessen, L. van der Ham, H. van den Berg, Electrochemical conversion of carbon dioxide to ethylene: plant design, evaluation and prospects for the future, Chemical Engineering Research and Design 182 (2022) 194-206. https://doi.org/10.1016/j.cherd.2022.03.034.
[72] G.P. Towler, R.K. Sinnott, Chemical engineering design : principles, practice, and economics of plant and process design, 2nd ed., Oxford ; Waltham2013.
[73] Nickel Price (USD / Kilogram) Chart for the Last 3 Months. https://www.dailymetalprice.com/metalpricecharts.php.
[74] W. Ma, G. Jacobs, D.E. Sparks, B. Todic, D.B. Bukur, B.H. Davis, Quantitative comparison of iron and cobalt based catalysts for the Fischer-Tropsch synthesis under clean and poisoning conditions, Catalysis Today 343 (2020) 125-136. https://doi.org/https://doi.org/10.1016/j.cattod.2019.04.011.
[75] A. Christensen, Assessment of Hydrogen Production Costs from Electrolysis: United States and Europe, 2020.
[76] EMBER, Carbon Price Tracker.
[77] E.R. Morgan, J.F. Manwell, J.G. McGowan, Opportunities for economies of scale with alkaline electrolyzers, International Journal of Hydrogen Energy 38(36) (2013) 15903-15909. https://doi.org/https://doi.org/10.1016/j.ijhydene.2013.08.116.
[78] H. Van 't Noordende , P. Ripson, A One-GigaWatt Green-Hydrogen Plant 2022.
[79] A.O. Oni, K. Anaya, T. Giwa, G. Di Lullo, A. Kumar, Comparative assessment of blue hydrogen from steam methane reforming, autothermal reforming, and natural gas decomposition technologies for

natural gas-producing regions, Energy Conversion and Management 254 (2022) 115245. https://doi.org/https://doi.org/10.1016/j.enconman.2022.115245.
[80] D. Mehanovic, A. Al-Haiek, P. Leclerc, D. Rancourt, L. Fréchette, M. Picard, Energetic, GHG, and economic analyses of electrified steam methane reforming using conventional reformer tubes, Energy Conversion and Management 276 (2023) 116549. https://doi.org/https://doi.org/10.1016/j.enconman.2022.116549.
[81] P. Sulewski, W. Ignaciuk, M. Szymańska, A. Wąs, Development of the Biomethane Market in Europe, Energies 16(4) (2023) 2001. https://doi.org/10.3390/en16042001.
[82] Deloitte, Fueling the future of mobility: hydrogen electrolyzers, 2021.
[83] OPEC, OPEC Basket Price. https://www.opec.org/opec_web/en/data_graphs/40.htm. (Accessed 12/12 2023).
[84] C. Choe, S. Cheon, J. Gu, H. Lim, Critical aspect of renewable syngas production for power-to-fuel via solid oxide electrolysis: Integrative assessment for potential renewable energy source, Renewable and Sustainable Energy Reviews 161 (2022) 112398. https://doi.org/10.1016/j.rser.2022.112398.
[85] H. Shin, D. Jang, S. Lee, H.-S. Cho, K.-H. Kim, S. Kang, Techno-economic evaluation of green hydrogen production with low-temperature water electrolysis technologies directly coupled with renewable power sources, Energy Conversion and Management 286 (2023) 117083. https://doi.org/10.1016/j.enconman.2023.117083.
[86] N. Heck, C. Smith, E. Hittinger, A Monte Carlo approach to integrating uncertainty into the levelized cost of electricity, The Electricity Journal 29(3) (2016) 21-30. https://doi.org/https://doi.org/10.1016/j.tej.2016.04.001.
[87] IRENA, Renewable power generation costs in 2022, in: I.R.E. Agency (Ed.) Abu Dhabi., 2023.
[88] Z. Wang, W. Wang, W. Qin, W. Gui, S. Xu, C. Yang, Z. Zhang, Y. Wang, J. Zheng, X. Liu, Analysis of carbon footprint reduction for three novel air separation columns, Separation and Purification Technology 262 (2021) 118318. https://doi.org/https://doi.org/10.1016/j.seppur.2021.118318.
[89] S. Cho, W. Noh, I. Lee, Hybrid systems design for blue and green hydrogen co-production: Integration of autothermal reforming with solid oxide electrolysis, Energy Conversion and Management 300 (2024) 117969. https://doi.org/https://doi.org/10.1016/j.enconman.2023.117969.